Study and optimisation of the common mode exploitation for xDSL application

Vincent Le Nir, Marc Moonen

Abstract

This report explains how the common mode can be exploited in order to increase the capacity of xDSL systems in a binder MIMO channel. Indeed, N copper pairs can use either differential or/and common modes to transmit N or (2N-1) signals. At the receiver side, the common mode can be used to mitigate RFI or/and transmit additional data signal. However, some care should be taken with egress. A channel model is proposed including differential and common mode channels, balanced functions for the leakage between common and differential modes, NEXT and FEXT both in common and differential modes. For coordinated or uncoordinated transmitters and receivers, results show that using the common mode provide better results in terms of capacity and/or performance than traditional differential mode.

Index Terms

Differential mode, common mode, phantom mode, egress, VDSL, MIMO

I. Introduction

The growing demand for high speed services like video on demand, peer-to-peer sharing and High Definition TeleVision (HDTV) call for new paradigms increasing the capacity and the performance. For instance, Very-high data-rate Digital Subscriber Line (VDSL) transmit data in a 12 or 30 MHz bandwidth compared to the former 1 MHz for Asymetric DSL (ADSL) [1]. However, the magnitude of the channel transfert function decreases with frequency while crosstalk (NEXT and FEXT) can increase depending on the length of the line and the frequency [2]. Therefore, new transmitters and receivers needs to be developped for these binder Multiple Input Multiple Output (MIMO) channels. For coordinated transmitters and receivers, the optimal solution is based on the Singular Value Decomposition (SVD) of the MIMO channel [3], [4]. With coordination only at the receiver or the transmitter side, the optimal solution was found to be the Decision Feedback Canceller (DFE) or dirty paper coding (Harashima precoder based on DFE on multi-user interference) [5]. So far, the optimal solution for uncoordinated transmitters and receivers uses Dynamic Spectrum Management (DSM) [6], [7], [8], [9], [10], [11], [12], [13]. Increasing the frequency band is not the only way to increase the capacity and performance. Recently, the exploitation of the common mode was used to mitigate Radio Frequency Interference (RFI) signals [14], [15] or crosstalk signals [16], [17] for a single pair. The later article showed that the common mode channel has less attenuation than the differential mode channel. It was also proven that the use of the common mode leads to an higher capacity system than the differential mode [18], [19], [20], [21], [22]. Moreover, [23], [24] demonstrated that for a binder MIMO channel, both wires of a pair can be used to transmit information. Indeed, with N pairs and by setting one wire as the ground, it is possible to transmit (2N-1) signals. In this article, we propose to use both differential and common modes to transmit (2N-1) signals in a binder MIMO channel of N pairs in a symmetric way to exploit the properties of the common mode channel. A new channel model is proposed since the common mode is excited, and leaks from the common to the differential mode at the transmitting end with the Longitudinal Conversion Loss (LCL) and at the far end with the Longitudinal Conversion Transfer Loss (LCTL). The leakage from differential to common mode is called Transverse Loss Conversion (TCL) at the transmitting end and Transverse Conversion Transfer Loss (TCTL) at the receiving end [25]. Then performance results are given using the different SVD, DFE or DSM algorithms with different cases of coordination or uncoordination between transmitters and receivers. The issue of transmit Power Spectrum Density (PSD) and egress is also adressed.

II. Channel Model

A. Differential-Mode

The channel model for 24 American Wire Gauge (AWG) twisted pairs in the differential-mode is given by the two-port model with resistance $R(f)$, inductance $L(f)$, conductance $G(f)$ and capacitance $C(f)$ as shown in Figure 1 where $X(f)$ is the transmitted signal and $Y(f)$ is the received signal. The channel $H(f)$ is computed as the ratio between $Y(f)$ and $X(f)$. The $RLCG$ components are computed as follows for a 24 AWG [17]:

$$R(f) = (174.55888^4 + 0.053073481 f^2)^{1/4} \Omega/km \tag{1}$$

$$L(f) = \frac{617.29539 + 478.97099 \left(\frac{f}{553760}\right)^{1.1529766}}{1 + \left(\frac{f}{553760}\right)^{1.1529766}} \mu H/km \tag{2}$$

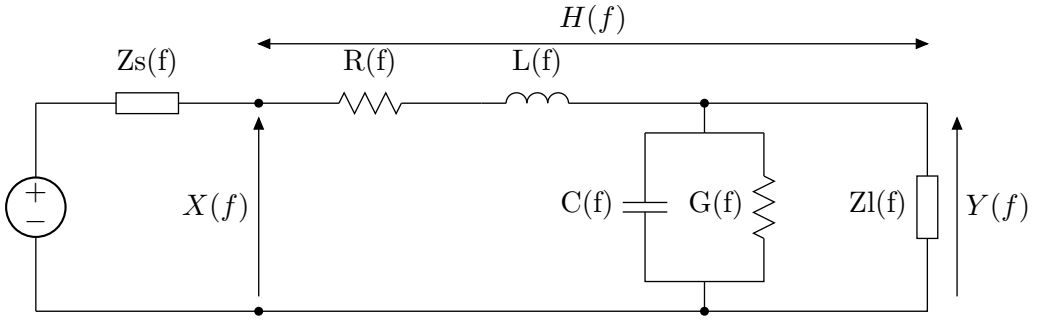

Fig. 1. Line theory R, L, C, G representation for an incremental section dx of a telephone line

$$G(f) = 234.87476 f^{1.38} fS/km \tag{3}$$

$$C(f) = 50nF/km \tag{4}$$

These parameters lead to the propagation matrix $\gamma(f)$ and the characteristic impedance $Z_0(f)$ which are computed as:

$$\gamma(f) = \sqrt{(R(f) + 2\pi jfL(f))(G(f) + 2\pi jfC(f))} m^{-1} \tag{5}$$

$$Z_0(f) = \frac{(R(f) + 2\pi jfL(f))}{(G(f) + 2\pi jfC(f))} \Omega \tag{6}$$

The values of $Z_0(f)$ vary between 100 Ω and 110 Ω. Therefore the load impedance $Z_L(f)$ is set to Z_L =100 Ω, giving the following formula for the differential-mode channel depending on the length of the line (d in meters) [26]:

$$H(f) = \frac{Z_L}{cosh(\gamma(f)d)Z_L + Z_0(f)sinh(\gamma(f)d)} \tag{7}$$

B. Common-Mode

The common mode channel is computed using the differential-mode channel with different parameters $R(f)$, $L(f)$, $C(f)$, $G(f)$. Indeed, the observations from [17] and previous articles showed that differential-mode and common-mode parameters are related using the following formulas:

$$R_c(f) = 0.55R(f) \tag{8}$$

$$L_c(f) = 4.4L(f) \tag{9}$$

$$G_c(f) = 2G(f) \tag{10}$$

$$C_c(f) = 0.95C(f) \tag{11}$$

However, as the characteristic impedance in the common-mode varies between 210 Ω and 240 Ω, the load impedance in the common-mode is set to 210 Ω. Figure 2 shows the attenuation of the Differential-Mode (DM) and the Common-Mode (CM) with frequencies up to 30 MHz. This results shows that the CM channel is less attenuated than the DM channel due to its lower resistance which is twice as less than the DM. The following Figures 3 show the attenuation of the DM and the CM channels respectively according to the length of the cable (d) varying form 0 to 1 kilometer. Obviously, the attenuation of the DM and the CM channels decrease with frequency and the length of the cable. One can notice that for 1 km cable at 30 MHz, the difference between the DM channel attenuation and the CM channel attenuation is 80 dB.

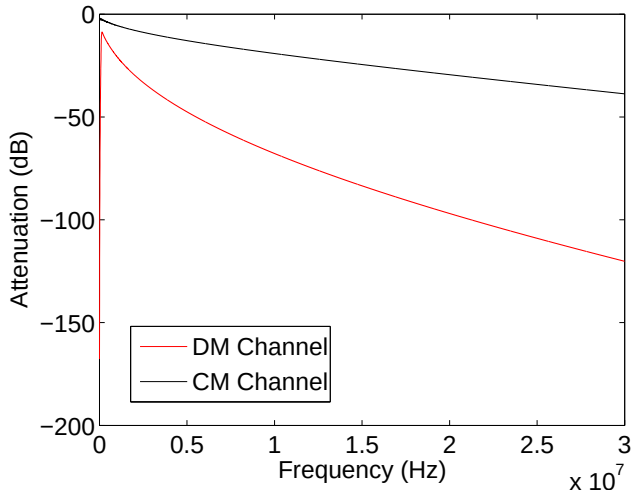

Fig. 2. Comparison between Differential-Mode (DM) and Common-Mode (CM) Attenuations with frequency

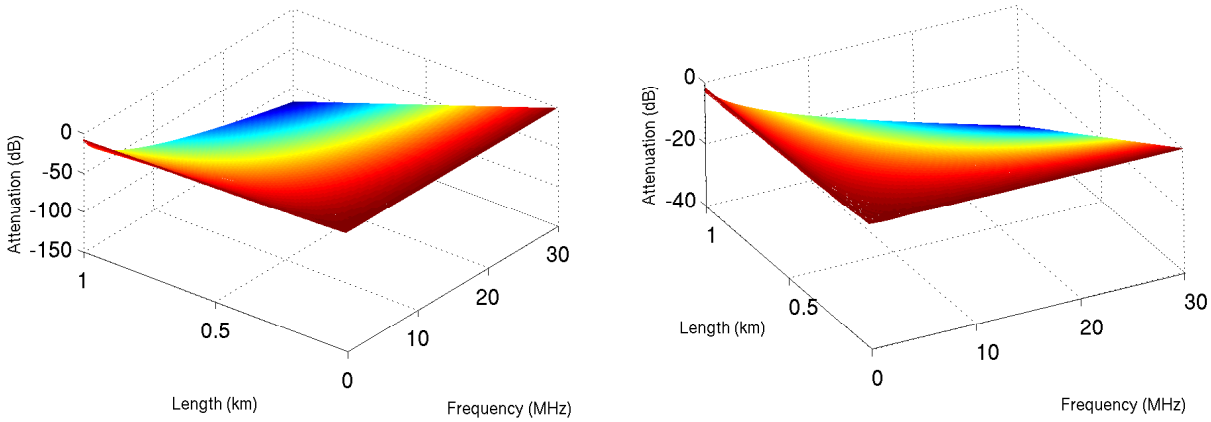

Fig. 3. Differential-Mode (DM) (left side) and Common-Mode (CM) (right side) Attenuations with frequency and the length of the cable

C. Mixing Differential-Mode and Common-Mode channel by the balance function

The DM and CM channels are not decorrelated. Indeed, when a voltage is transmitted in the DM, some of it goes in the CM and conversely. For the literature using the CM for interference cancellation [17], the most important balance function is the function that goes from the DM to the CM at the receiving end or Transverse Conversion Transfer Loss (TCTL) because of the lower attenuation in the CM compared to the DM. However, this literature does not transmit data in the CM. When data is transmitted both in the DM and the CM, the Longitudinal Conversion Transfer Loss (LCTL) from the CM to the DM at the receiving end, the Longitudinal Conversion Loss (LCL) from the CM to the DM at the transmitting end and the Transverse Conversion Loss (TCL) from the DM to the CM at the transmitting end should be considered.

The equivalent channel will consider all these different balance functions when transmitting data in the CM and the DM. The DM channel is determined by the variable h_d. The CM channel is determined by the variable h_c. The inverse of the TCTL balance function is determined by the variable h^r_{d2c}. The inverse of the LCTL balance function is determined by the variable h^r_{c2d}. The inverse of the TCL balance function is determined by the variable h^t_{d2c}. The inverse of the LCL balance function is determined by the variable h^t_{c2d}.

The equivalent channel representation is given by Figure 4 where all the balanced functions which make leakage from one mode to the other are shown. At the transmitter side, the leakage does not depend on DM and CM channel characteristics. At the receiver side, the leakage from CM to DM and DM to CM is also dependent on the DM and CM channel characteristics since this leakage can occur everywhere along the line. The equivalent channel can be determined by the multiplication of 3 matrices

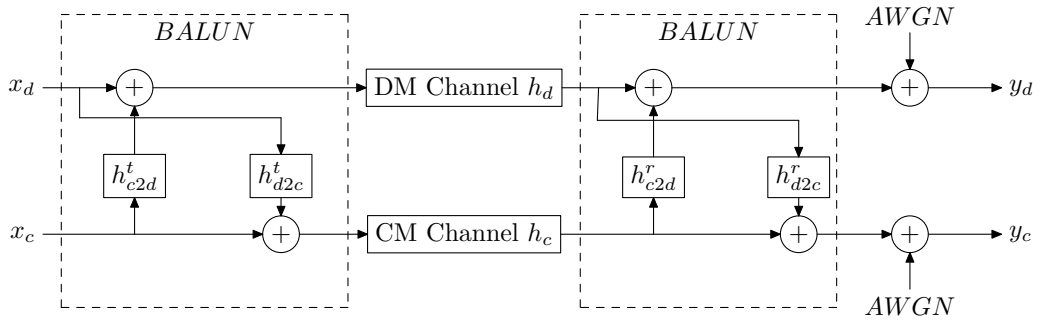

Fig. 4. Equivalent channel representation of a mixed DM and CM channel with leakage from one mode to the other at the transmitter and the receiver side

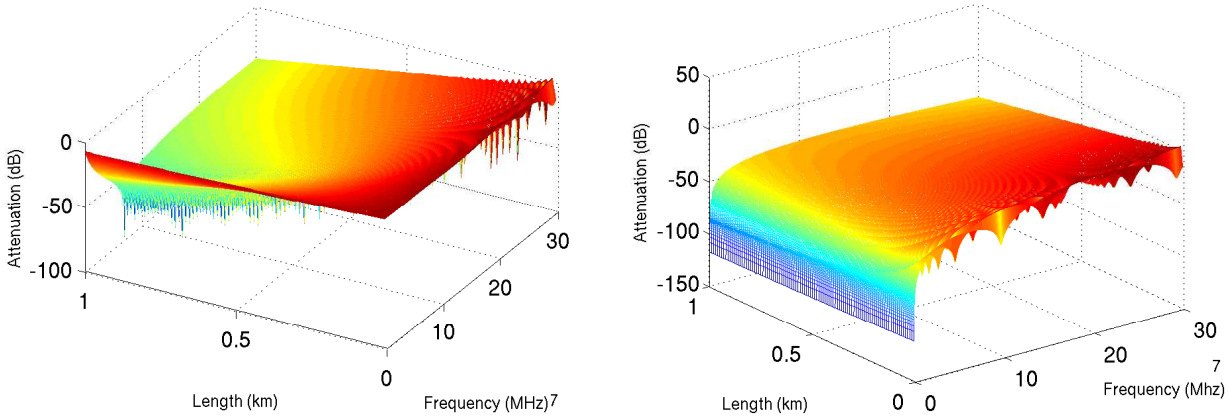

Fig. 5. Mixed DM and CM channels H^{11}_{eq} (left side) and H^{12}_{eq} (right side)

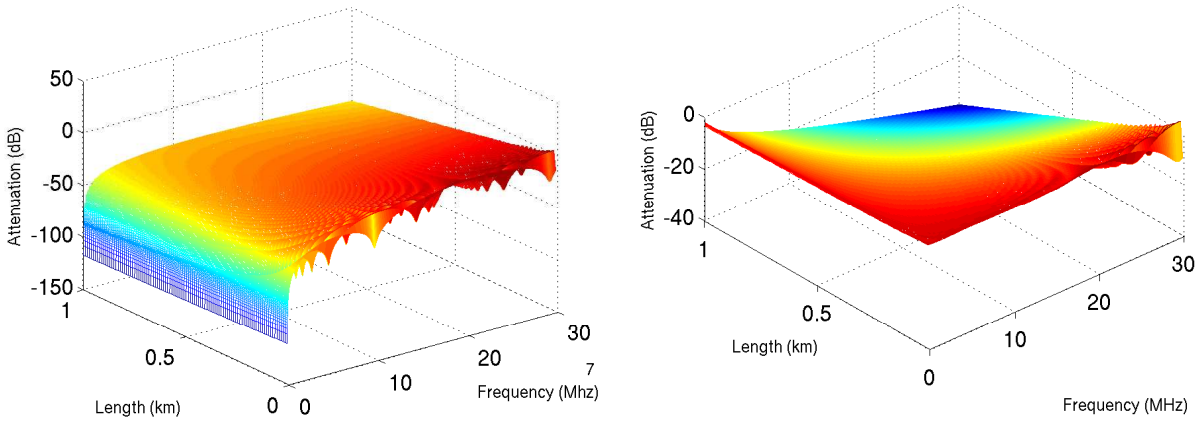

Fig. 6. Mixed DM and CM channels H^{12}_{eq} (left side)and H^{22}_{eq} (right side)

$$H_{eq} = \begin{bmatrix} 1 & h^r_{c2d} \\ h^r_{d2c} & 1 \end{bmatrix} \quad \begin{bmatrix} h_d & 0 \\ 0 & h_c \end{bmatrix} \quad \begin{bmatrix} 1 & h^t_{c2d} \\ h^t_{d2c} & 1 \end{bmatrix} \tag{12}$$

This leads to the following matrix :

$$H_{eq} = \begin{bmatrix} h_d + h^t_{d2c} h_c h^r_{c2d} & h^t_{c2d} h_d + h_c h^r_{c2d} \\ h_d h_{d2c} r + h^t_{d2c} h_c & h^t_{c2d} h_d h^r_{d2c} + h_c \end{bmatrix} \tag{13}$$

$$H_{eq} = \begin{bmatrix} H^{11}_{eq} & H^{12}_{eq} \\ H^{21}_{eq} & H^{22}_{eq} \end{bmatrix} \tag{14}$$

In order to test this mixed CM and DM channel, the inverse of the TCTL balance function for Category 3 pairs was chosen for h^r_{d2c}. Moreover, we set $h^r_{d2c} = h^r_{c2d} = h^t_{d2c} = h^t_{c2d}$. The TCTL balance function is equal to:

$$B(f) = \begin{cases} \sqrt{10^5} & 0 \leq f \leq 150kHz \\ \sqrt{10^5 \left(\frac{15000}{f}\right)^{1.5}} & f > 150kHz \end{cases} \tag{15}$$

The following Figures 5, 6 show the attenuation of the equivalent channel of mixed DM and CM transmission channels H^{11}_{eq}, H^{12}_{eq}, H^{21}_{eq}, H^{22}_{eq} respectively according to the length of the cable (d) varying from 0 to 1 kilometer and frequency from 0 to 30 MHz.

D. Egress tradeoff between Differential-Mode and Common-Mode

The references [27], [28] give the acceptable level of egress in a differential-mode xDSL transmission. The voltage that goes into the common mode using a differential-mode transmission is:

$$V_{d2c} = \frac{\sqrt{PSD_d W Z_L}}{B} \tag{16}$$

where PSD_d is assumed flat over the bandwidth W, Z_L is the load impedance of the line in differential-mode and B is the balance function between DM and CM.

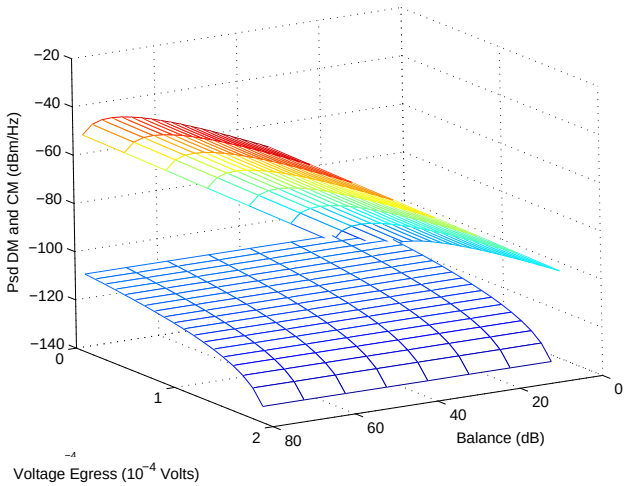

Fig. 7. Acceptable PSD in DM and CM for the maximum voltage of 0.2 mV of egress

The limit of the voltage of common mode is 0.2 mV in HAM bands. Therefore, when using the common-mode for transmission, some care should be taken with the PSD in the common-mode PSD_c. The voltage induced by the common-mode PSD is:

$$V_c = \sqrt{PSD_c W Z^c_L} \tag{17}$$

where Z^c_L is the load impedance in the common-mode. The total voltage in the common-mode is:

$$V_{CM} = V_{d2c} + V_c \tag{18}$$

Figure 7 shows the acceptable levels that should be put on the CM and on the DM not to overtake the particular treshold of 0.2 mV for egress in HAM bands of 10 kHz with $Z_L = 100$ Ohms and $Z_L^c = 210$ Ohms. As can be seen on the figure, the PSD for the common-mode transmission should be low compared to the differential mode. However, in non-HAM bands, it is possible to have more than 0.2 mV for egress, and knowing that spectral masks for VDSL can be up to -40 dBm/Hz, a trade-off between PSD in the DM and PSD in the CM should be considered.

III. Capacity

In VDSL technology, the theoretical capacity is given by the Schannon's equation:

$$C = \sum_{i=1}^{N_c} log_2(1 + \frac{\rho}{\Gamma}|h_i|^2) \tag{19}$$

with N_c the number of subcarriers, ρ the Signal to Noise Ratio (SNR) and Γ the loss factor depending on the target Bit Error Rate (BER), the margin and the coding gain. Assuming a Power Spectral Density of the signal of -60 dBm/Hz and an AWGN noise of -140 dBm/Hz, a target BER of 10^{-7} giving a -9.8 dB efficiency according to the specifications of VDSL, a margin of -6 dB and a coding gain of 3.8 dB, this gives a SNR of 80 dB and a loss factor of 12 dB. Figure 8 (left side) shows the data rate for a VDSL differential-mode transmission from 0 to 30 MHz with 4 kHz subcarriers and a load impedance of 100 Ω.

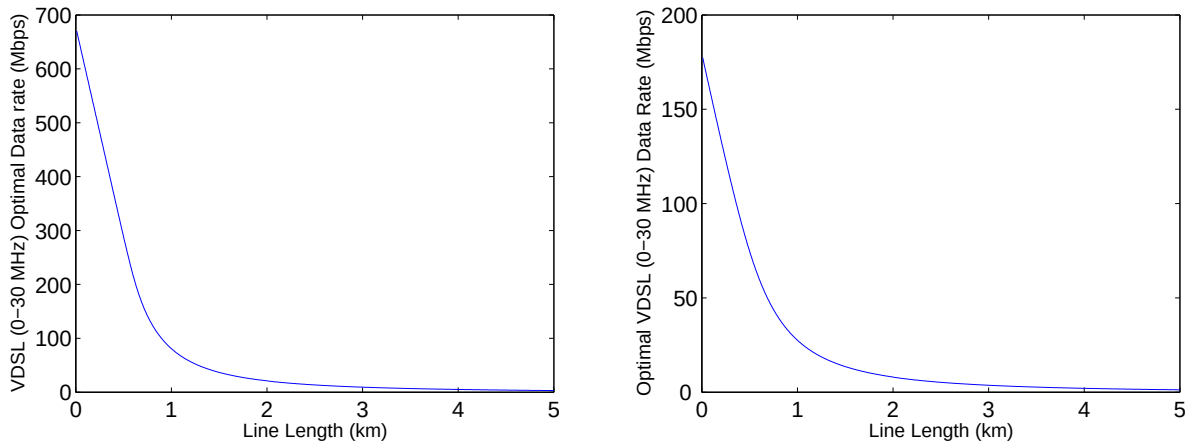

Fig. 8. Optimal Data Rate of a VDSL differential-mode (left side) and common-mode (right side) transmission 0-30 MHz with PSD -60 dBm/Hz (DM) and -110 dBm/Hz (CM)

For a VDSL common-mode transmission some care should be taken with egress particularly in HAM bands. Therefore the PSD is set to -110 dBm/Hz with an AWGN noise of -140 dBm/Hz, giving a SNR of 30 dB with the same factor loss of 12 dB. Figure 8 (right side) shows the data rate for a VDSL common-mode transmission from 0 to 30 MHz with 4 kHz subcarriers and a load impedance of 210 Ω.

For a mixed transmission in VDSL between differential-mode and common-mode, the balanced function should be taken into account by the equivalent channel matrix:

$$H_{eq} = \begin{bmatrix} h_d + h_{d2c}^t h_c h_{c2d}^r & h_{c2d}^t h_d + h_c h_{c2d}^r \\ h_d h_{d2c}^r + h_{d2c}^t h_c & h_{c2d}^t h_d h_{d2c}^r + h_c \end{bmatrix} \tag{20}$$

In order to test this mixed CM and DM channel, the inverse of the TCTL balance function for Category 3 pairs was chosen for h_{d2c}^r. Moreover, we set $h_{d2c}^r = h_{c2d}^r = h_{d2c}^t = h_{c2d}^t$. The TCTL balance function is equal to:

$$B(f) = \begin{cases} \sqrt{10^5} & 0 \leq f \leq 150kHz \\ \sqrt{10^5 \left(\frac{15000}{f}\right)^{1.5}} & f > 150kHz \end{cases} \tag{21}$$

The channel capacity for this mixed transmission becomes:

$$C = \sum_{i=1}^{N_c} log_2[det(I_2 + \frac{\Theta}{\Gamma} H_{eq}^H H_{eq})] \tag{22}$$

with $\Theta = diag(\rho_d, \rho_c)$.

Figure 9 shows the data rate for a VDSL differential-mode transmission from 0 to 30 MHz with 4 kHz subcarriers and a load impedance of 100 Ω for differential-mode and 210 Ω for common-mode. Here $\rho_d = 80dB$ and $\rho_c = 30dB$. The curve "DM+CM uncorrelated" represent the addition of the differential-mode and the common-mode as if there was no leakage from one mode to the other. Therefore $H_{eq}^H H_{eq} = diag(|h_d|^2, |h_c|^2)$. The curve "DM+CM correlated" represents the differential-mode and common-mode transmission which are related by the balance function. One can observe that for a particular small length of line, the correlated system provides higher data rates than the addition of both modes.

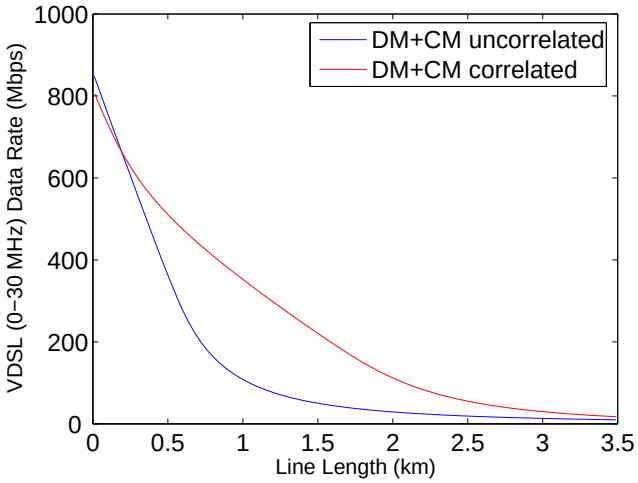

Fig. 9. Optimal Data Rate of a VDSL mixing differential-mode and common-mode transmission 0-30 MHz with PSD_d=-60 dBm/Hz and PSD_c =-110 dBm/Hz

IV. Crosstalk NEXT and FEXT limitations

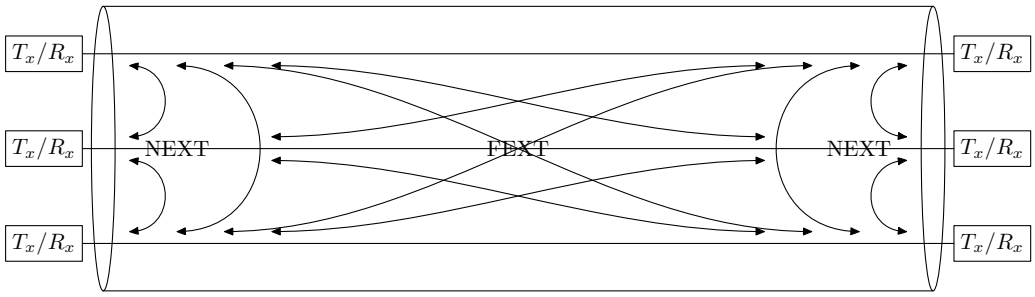

Fig. 10. Graphical representation of FEXT and NEXT in a multi-pair system

A representation of Near End Crosstalk (NEXT) and Far End Crosstalk (FEXT) for a multi-pair system is given in Figure 10. In a multi-pair system, it is necessary to have good theoretical tools to predict the effect of NEXT and the FEXT [29], [30], [31], [32]. The 1% worst case model for NEXT and FEXT in the differential mode give the following equations for N disturbers in a 50 twisted-pair bundle [17]:

$$PSD_d^{NEXT}(f) = PSD_d^{Disturber}(f) \left(\frac{N}{49}\right)^{0.6} 10^{-13} f^{1.5} \tag{23}$$

$$PSD_d^{FEXT}(f) = PSD_d^{Disturber}(f)|h_d(f)|^2 \left(\frac{N}{49}\right)^{0.6} 9.10^{-20} df^2 \tag{24}$$

Figure 11 shows the loop attenuation of a 1 km cable in the differential-mode, as well as NEXT and FEXT in the differential-mode according to the previous equations. One can see that the NEXT is more powerful than FEXT but can be avoided using FDD or TDD transmission. For a 1 km cable, we can see that FEXT follows the contribution of the loop attenuation more than the square of the frequency.

Figures 12 show the NEXT and FEXT of a differential-mode against frequency and line length between 0 and 1 km. One can see that NEXT is constant against line length but FEXT is varying depending on the length of the cable. Indeed, for short

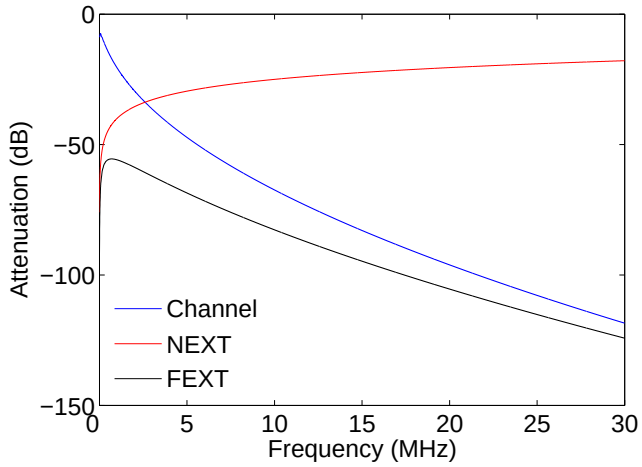

Fig. 11. Loop Attenuation, NEXT and FEXT for 1 km cable in differential-mode

loop lengths, FEXT is increasing with frequency following the f^2 contribution, but as the loop length increases, FEXT is following the $|h_d(f)|^2$ contribution and therefore is decreasing with frequency.

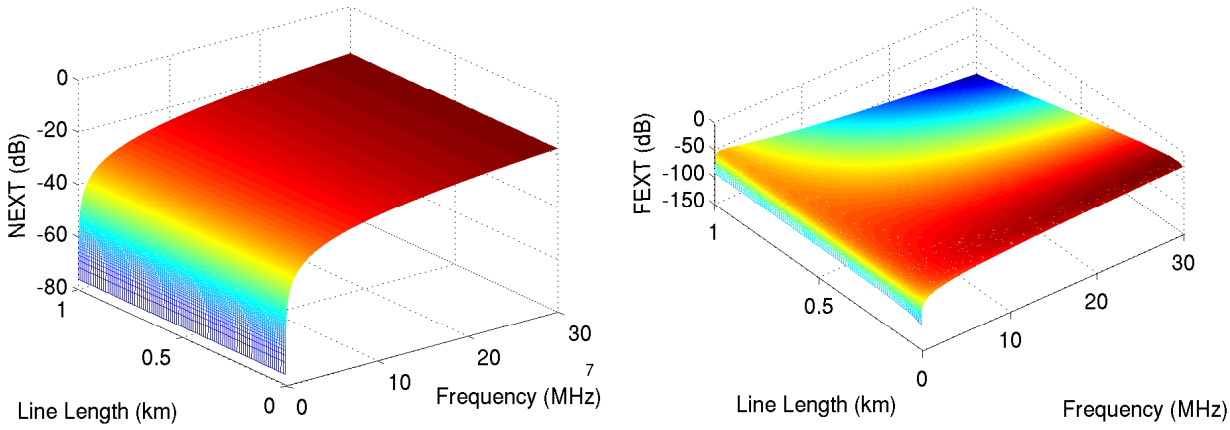

Fig. 12. NEXT (left side) and FEXT (right side) as a function of line length and frequency in differential-mode

For common-mode transmission, there is no model available as for differential-mode transmission. Since NEXT doesn't depend on line length and channel attenuation, the NEXT in common-mode is comparable to the NEXT in differential-mode. However, FEXT does depend on line length and channel attenuation, and since the channel attenuation in common-mode is stronger than channel attenuation in differential-mode, the FEXT will be stronger in common-mode than in differential-mode at the receiver. Since there is no model available for NEXT and FEXT in the CM, we take the equations of NEXT and FEXT in the DM with the CM propagation channel. This leads to :

$$PSD_c^{NEXT}(f) = PSD_c^{Disturber}(f)\left(\frac{N}{49}\right)^{0.6} 10^{-13} f^{1.5} \tag{25}$$

$$PSD_c^{FEXT}(f) = PSD_c^{Disturber}(f)|h_c(f)|^2\left(\frac{N}{49}\right)^{0.6} 9.10^{-20} df^2 \tag{26}$$

Figure 13 shows the loop attenuation of a 1 km cable in the common-mode, as well as NEXT and FEXT in the common-mode according to the previous equations. Figures 14 show the NEXT and FEXT of a common-mode against frequency and line length between 0 and 1 km. The NEXT equation is the same as for differential-mode. For FEXT, we notice that the attenutation is less prononced than FEXT in the differential-mode due to the contribution of the common-mode channel. However, as for

differential-mode, for short loop lengths, FEXT is increasing with frequency following the f^2 contribution, but as the loop length increases, FEXT is following the $|h_c(f)|^2$ contribution and therefore is decreasing with frequency.

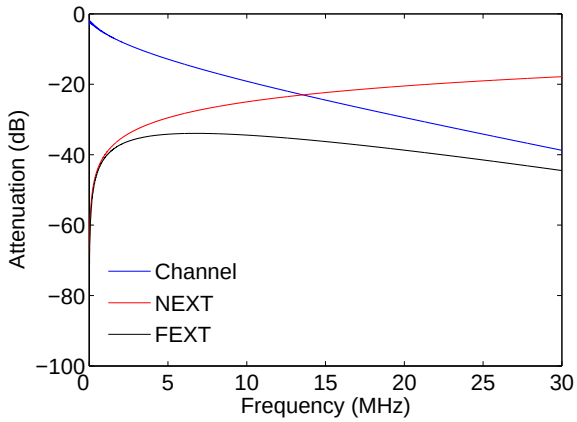

Fig. 13. Loop Attenuation, NEXT and FEXT for a 1 km cable in a common-mode transmission

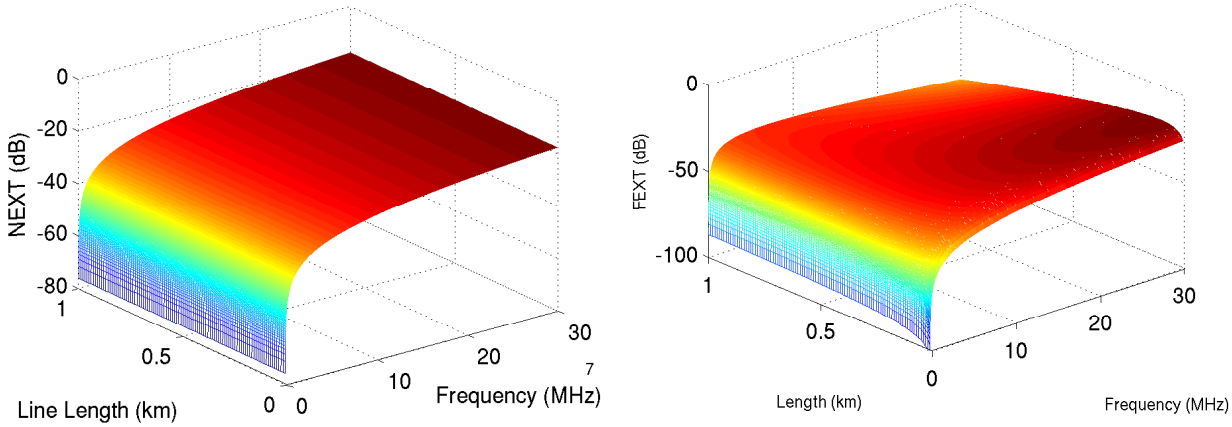

Fig. 14. NEXT (left side) and FEXT (right side) as a function of line length and frequency in common-mode

V. Capacity with crosstalk for DM and CM transmission

For a DM transmission with FEXT, the capacity formula becomes for the DM of user k:

$$C = \sum_{i=1}^{N_c} log_2(1 + \frac{PSD_d}{\Gamma(\sum_{n \neq k} |h_d^{n,i}|^2 + \sigma_k)} |h_d^{k,i}|^2) \tag{27}$$

with σ_k the PSD of the noise. The capacity formula for the CM transmission of user k is:

$$C = \sum_{i=1}^{N_c} log_2(1 + \frac{PSD_c}{\Gamma(\sum_{n \neq k} |h_c^{n,i}|^2 + \sigma_k)} |h_c^{k,i}|^2) \tag{28}$$

Figure 15 show the data rate performance of separated DM (left side) and CM (right side) with $PSD_d = -60$ dBm/Hz and $PSD_c = -110$ dBm/Hz and a PSD for the noise equal to -140 dBm/Hz. One can see that for short loops in the DM and the CM, the data rate decreases compared to the system without FEXT. When the length of the line increases, there is no need to cope with FEXT disturbers by particular algorithms.

The capacity of mixed DM and CM transmission with FEXT is given by:

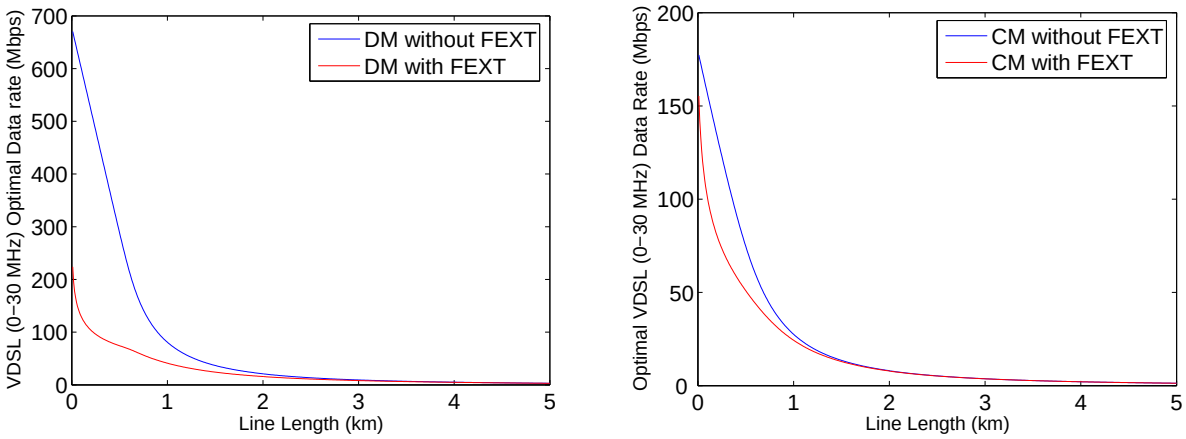

Fig. 15. Capacity performance in presence of FEXT disturbers for the DM (left side) and the CM (right side) transmission

$$C = \sum_{i=1}^{N_c} log_2[det(I_2 + \frac{\Theta}{\Gamma} H_{eq}^H H_{eq})] \tag{29}$$

with $\Theta = diag(\frac{PSD_d}{(\sum_{n \neq k} |h_d^{n,i}|^2 + \sigma_k)}, \frac{PSD_c}{(\sum_{n \neq k} |h_c^{n,i}|^2 + \sigma_k)})$.

Figure 16 shows the data rate performance of mixed DM and CM with $PSD_d = -60$ dBm/Hz and $PSD_c = -110$ dBm/Hz and a PSD for the noise equal to -140 dBm/Hz. As for previous figures the exploitation of FEXT provide a gain with data rate for short loops. The interesting thing about this figure is that when using a mixed mode between CM and DM with FEXT the data rate is almost 4 times higher for 1 km loop than the addition of uncorrelated DM and CM.

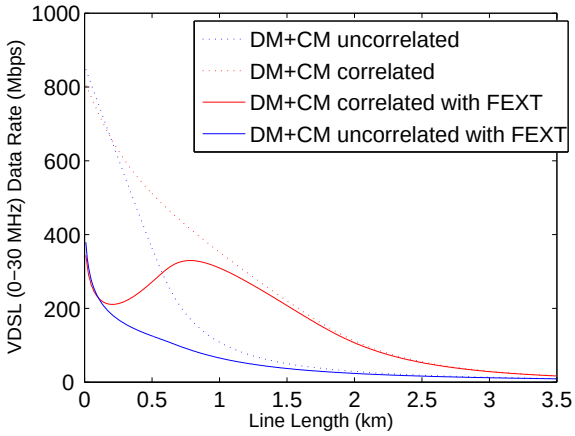

Fig. 16. Capacity performance in presence of FEXT disturbers for the mixed DM and CM transmission

VI. NEXT AND FEXT LEAKAGE

In the previous section, we have considered a separated NEXT and FEXT for the CM and the DM. However, there is some leakage of the FEXT and NEXT from the DM to the CM and conversely. In the previous literature, the leakge from the DM to the CM was only considered because no data was transmitted on the CM. This literature considered the Balance function :

$$B(f) = \begin{cases} \sqrt{10^5} & 0 \leq f \leq 150kHz \\ \sqrt{10^5 \left(\frac{15000}{f}\right)^{1.5}} & f > 150kHz \end{cases} \tag{30}$$

The NEXT and FEXT leakage from the differential-mode to the common-mode was formulated in [16] as:

$$PSD_c^{NEXT}(f) = PSD_d^{NEXT}(f) B(f) \tag{31}$$

$$PSD_c^{FEXT}(f) = PSD_d^{FEXT}(f)B(f)e^{j(\lfloor h_c - \lfloor h_d)} \tag{32}$$

One year later, the same author gave two new formulas for the leakage from the differential-mode to Common-mode NEXT and FEXT [17]:

$$PSD_c^{NEXT}(f) = PSD_d^{NEXT}(f)gain\frac{1}{\sqrt{|B(f)|h_c|(f)|}} \tag{33}$$

where $gain$ is adjusted to have the same overall NEXT output level as in differential mode.

$$PSD_c^{FEXT}(f) = PSD_d^{FEXT}(f)|h_c(f)|B(f)e^{j(\lfloor h_c - \lfloor h_d)} \tag{34}$$

In [20], Magesacher did some measurements of the leaked CM FEXT and found that leaked CM FEXT is at least as strong as the DM FEXT, depending on the frequency range, up to 10 dB stronger. In the proposed model, we consider the leakage from the CM to the DM like the channel propoagation. Because of the TDD or FDD transmission, we focus on FEXT. Contrary to the channel model, the leakage from the DM to the CM and from the CM to the DM appear on the line, therefore there is no leakage at the transmitter side and leads to the following matrix between FEXT voltages on the CM and the DM:

$$\begin{bmatrix} 1 & h_{c2d}^r \\ h_{d2c}^r & 1 \end{bmatrix} \tag{35}$$

In order to test this mixed CM and DM FEXT, the inverse of the TCTL balance function for Category 3 pairs $B(f)$ was chosen for h_{d2c}^r. Moreover, we set $h_{d2c}^r = h_{c2d}^r$. Therefore, our model leads to the following equations for FEXT:

$$PSD_{DM}^{FEXT}(f) = PSD_d^{FEXT}(f) + \frac{PSD_c^{FEXT}}{B(f)} \tag{36}$$

$$PSD_{CM}^{FEXT}(f) = PSD_c^{FEXT}(f) + \frac{PSD_d^{FEXT}}{B(f)} \tag{37}$$

Figure 17 shows the capacity in presence of mixed CM and DM FEXT as well as mixed CM and DM transmission. With TDD or FDD transmission to get rid of NEXT, this performance is likely the performance that could be observed in a real environment since leakage in both CM and DM for signal and crosstalk have been taken into account. The result prove that there is a lot to gain using crosstalk cancellation, especially in the mixed CM and DM scenario.

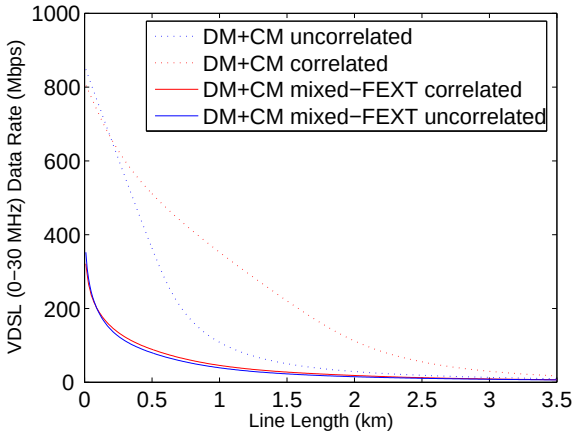

Fig. 17. Capacity performance in presence of mixed CM and DM FEXT disturbers for the mixed DM and CM transmission

Indeed, the next Figures 18 show the channel attenuation, the FEXT and the FEXT with leakage for an uncorrelated DM-CM system using a $PSD_d = -60$ dBm/Hz and $PSD_c = -110$ dBm/Hz and 1 km cable. It can be seen that the leakage from CM to DM is problematic for the differential-mode signal, since the power of the resultant FEXT is higher than the channel attenuation for high frequencies. Therefore, the assumption of Column Wise Diagonal Dominance (CWDD) or Row Wise Diagonal Dominance (RWDD) no longer exist for high frequencies in the differential mode. For the common-mode, the leakage from the CM to the DM is less problematic since the power of the resultant FEXT is not higher than the channel attenuation in CM, but we can note that there will be lower performance for low frequencies due to the leakage of DM.

The next Figures 19 show the channel attenuation, the FEXT and the FEXT with leakage for a mixed DM-CM system using a $PSD_d = -60$ dBm/Hz and $PSD_c = -110$ dBm/Hz and 1 km cable. As can be seen, the difference of PSD between the common-mode and the differential mode is problematic for the common-mode transmission, the leakage of the signal from the DM to the CM leads to a higher power than the transmission in the CM channel. However, for the FEXT the CWDD or RWDD still exist thanks to the leakage from the CM to the DM of the channel attenuation.

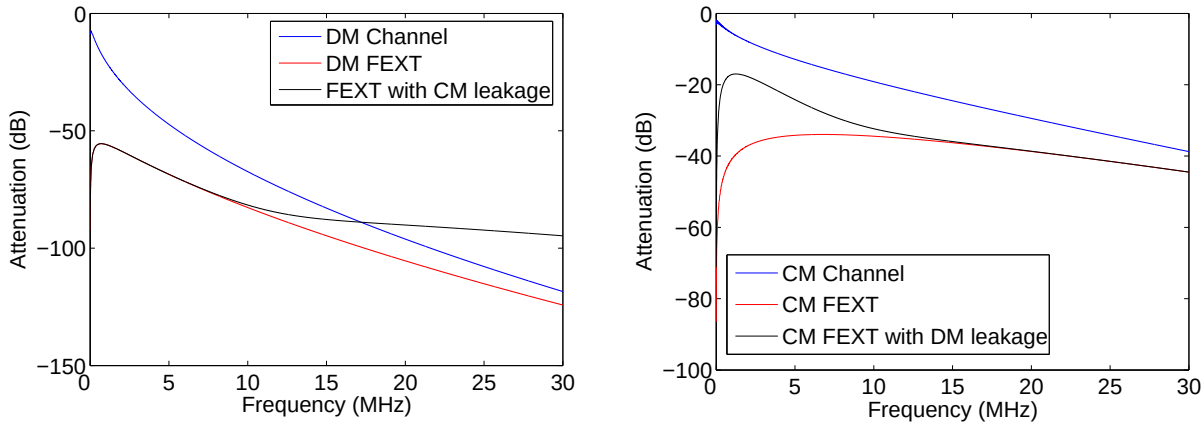

Fig. 18. Channel attenuation, FEXT and FEXT with leakage of the differential-mode transmission with $PSD_d = -60$ dBm/Hz and $PSD_c = -110$ dBm/Hz for a 1 km cable (left side) and Channel attenuation, FEXT and FEXT with leakage of the common-mode transmission with $PSD_d = -60$ dBm/Hz and $PSD_c = -110$ dBm/Hz for a 1 km cable (right side)

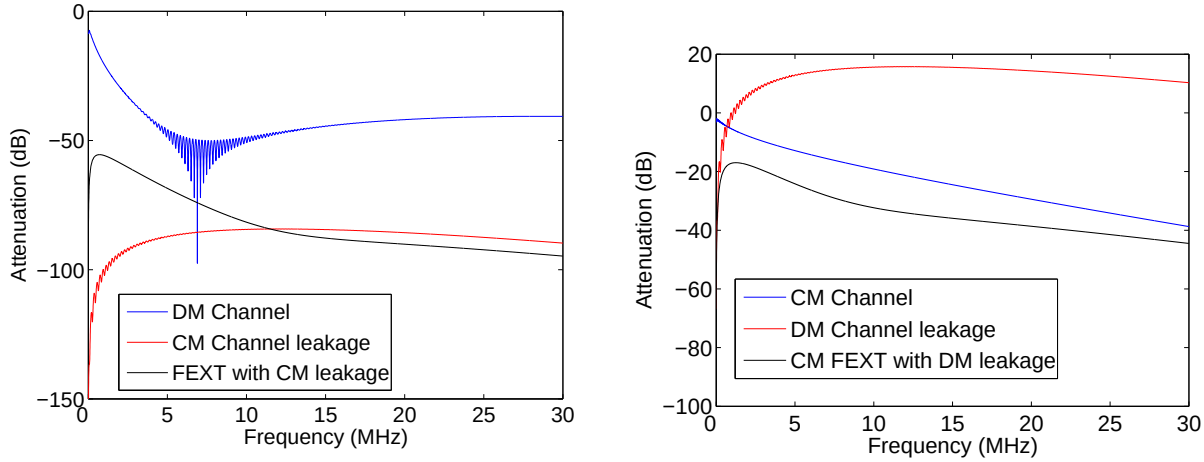

Fig. 19. Channel attenuation, CM Channel leakage and FEXT with CM leakage of the differential-mode transmission with $PSD_d = -60$ dBm/Hz and $PSD_c = -110$ dBm/Hz for a 1 km cable (left side) Channel attenuation, DM Channel leakage and FEXT with DM leakage of the common-mode transmission with $PSD_d = -60$ dBm/Hz and $PSD_c = -110$ dBm/Hz for a 1 km cable (right side)

VII. Maximum Capacity with egress limitations

Because the DM and CM channels are known at the transmitter side and the receiver side, there is no issue of co-location between DM and CM as it is the case for multi-user coordination. In order to achieve the maximum capacity, the powers on the DM and the CM must be chosen by the capacity formula for each subcarrier:

$$C = log_2[det(I_2 + \frac{\Theta}{\Gamma} H_{eq}^H H_{eq})] \tag{38}$$

$$C = log_2[det(I_2 + \frac{\Theta}{\Gamma} \Lambda)] \tag{39}$$

with $\Theta = diag(\rho_d, \rho_c)$ and $\Lambda = diag(\lambda_d, \lambda_c)$. To achieve the greatest possible capacity we must have:

$$PSD_d = \left(\mu - \frac{\sigma}{\lambda_d}\right)^+ \tag{40}$$

$$PSD_c = \left(\mu - \frac{\sigma}{\lambda_c}\right)^+ \tag{41}$$

Where μ is the water level. Furthermore μ should be chosen such that:

$$V_{CM} = V_{d2c} + V_c \tag{42}$$

does not exceed 0.2 mV for the egress in HAM bands with:

$$V_{d2c} = \frac{\sqrt{PSD_d WZ_L}}{B} \tag{43}$$

and

$$V_c = \sqrt{PSD_c WZ_L^c} \tag{44}$$

VIII. Conclusion

In this report we gave the differential-mode and common-mode channel model based on the two-port model. The results show that the CM channel is less attenuated than the DM channel. However, when data is transmitted trhough DM and CM channel simultaneously, no model is available in the literature. Therefore, we developed a mixed DM-CM channel model based on the different balance functions at the transmitting and the receiving end. Taking a known balance function, the different channel contributions were given. One major issue when transmitting both in the DM and the CM is the egress. Knowing that the worst-case is 0.2 mV in HAM bands, the acceptable PSD in the CM and the DM were given depending on the balance function. The results show that in HAM bands, the acceptable PSD in the CM should not exceed -110 dBm/Hz. Then, the maximum capacity for DM and CM transmission were given as well as the mixed DM-CM transmission. The results show that the mixed DM-CM transmission gives better results that the sum of separated DM and CM transmission because of the chosen balance function and the channel attenuation. This is mainly due to the weak channel attenuation of the common-mode and the weak balance function at high frequencies which are added to the DM channel, giving a weaker channel attenuation for the resulting DM channel. The capacity assumes channel knowledge at the receiver of the mixed DM-CM channel, which is true because any pair is colocated at the transmitter and the receiver. Higher capacities can be obtained using the water-filling scheme. When considering crosstalk NEXT and FEXT, the 1 $\%$ worst-case model was chosen for the DM. Since there is no model available for the CM, we chose to apply the DM equations to the CM with the CM channel. NEXT can be removed using TDD or FDD transmission. FEXT can be removed using algorithms like water-filling when there is colocation at the transmitter side and the receiver side, DFE or DFE precoding when there is colocation at only one side. However, a simple linear ZF has proven to provide 90 $\%$ of the maximal capacity even when there is no colocation betzeen transmitter and receivers. This is because of the RWDD or the CWDD of the DM FEXT matrix. In this report we gave the average capacity per user of a bundle of 50 pairs with FEXT for the CM and the DM separatly without using any algorithms. Because of crosstalk, the capacity decreases but less in the CM than the DM due to the low PSD in the CM (-110 dBm/Hz). Then the capacity with FEXT in the mixed DM-CM transmission was given. The capacity with FEXT reaches the capacity without FEXT for long line length. However, uncorrelated FEXT were used between the CM and the DM. As we know that power in the CM or the DM goes into the alternate mode by the balance function, the same phenomenum can be applied to FEXT. The leakage from the CM to the DM increases the FEXT level of the DM in high frequencies. The leakage from the DM to the CM increases the FEXT level of the CM in low frequencies. The final results give similar results for uncorrelated DM and CM transmission with FEXT and mixed DM-CM transmission with FEXT. However, the optimal capacity is higher in the mixed DM-CM transmission. When looking at the FEXT level compared to the channel attenuation, the FEXT level in the DM and in the CM is lower than the channel attenuation. That means that RWDD and CWDD is still applicable. However, there is no CWDD or RWDD between CM and DM channel matrix. Indeed, because of low PSD in the CM the DM channel leakage is much higher than the channel attenuation, meaning that it is neccesary to cope with the DM channel leakage. As CM and DM is obviously colocated at the transmitting end and the receiving end, a water-fillling scheme can be applied to the DM-CM channel matrix and CWDD or RWDD can be considered between pairs. Therefore, no colocation between pairs is needed and a simple linear ZF can be applied at the transmitter side or the receiver side to reach 90 $\%$ of the capacity like the DM transmission alone.

References

[1] W. Henkel, S. Olcer, K. S. Jacobsen, and B. R. Saltzberg, "Guest editorial twisted pair transmission-ever increqsing performances on ancient telephone wires," *IEEE Journal on Selected Areas in Communications*, vol. 20, no. 4, pp. 877–880, June 2002.

[2] G. Ginis and J. M. Cioffi, "Optimum bandwidth partitioning with analog-to-digital converter constraints," *IEEE Transactions on Communications*, vol. 52, no. 6, pp. 1010–1018, June 2004.

[3] G. Tauböck and W. Henkel, "Mimo systems in the subscriber-line network," in *5th International OFDM Workshop*, Hamburg, GERMANY, Sept. 2000, pp. 181–183.

[4] A. Ghobrial and R. Adhami, "Broadband communication in the access network," in *Communications in Computing*, Las Vegas, USA, June 2004.

[5] G. Ginis and J. M. Cioffi, "Vectored transmission for digital subscriber line systems," *IEEE Journal on Selected Areas in Communications*, vol. 20, no. 5, pp. 1085–1104, June 2002.

[6] S. Schelstraete, "Defining upstream power backoff for vdsl," *IEEE Journal on Selected Areas in Communications*, vol. 20, no. 5, pp. 1064–1074, June 2002.

[7] K. B. Song, S. T. Chung, G. Ginis, and J. M. Cioffi, "Dynamic spectrum management for next-generation dsl systems," *IEEE Communications Magazine*, pp. 101–109, Oct. 2002.

[8] W. Yu, "Distributed multiuser power control for digital subscriber lines," *IEEE Journal on Selected Areas in Communications*, vol. 20, no. 5, pp. 1105–1115, June 2002.

[9] B. Wiese and K. S. Jacobsen, "Use of the reference noise method bounds the performance loss due to upstream backoff," *IEEE Journal on Selected Areas in Communications*, vol. 20, no. 5, pp. 1075–1084, June 2002.

[10] R. Cendrillon, M. Moonen, R. Suciu, and G. Ginis, "Simplified power allocation and tx/rx structure for mimo-dsl," in *IEEE Global Telecommunications Conference (GLOBECOM)*, San Francisco, USA, Dec. 2003, pp. 1842–1846.

[11] R. Cendrillon, W. Yu, M. Moonen, J. Verlinden, and T. Bostoen, "Optimal multi-user spectrum management for digital subscriber lines," in *IEEE International Conference on Communications (ICC)*, Paris, FRANCE, June 2004.

[12] R. Cendrillon, "Multi-user signal and spectra co-ordination for digital subscriber lines," Ph.D. dissertation, Katholieke Universiteit Leuven, Dec. 2004.

[13] J. Lee, R. V. Sonalkar, and J. M. Cioffi, "A multi-user power control algorithm for digital subscriber lines," *IEEE Communications Letters*, vol. 9, no. 3, pp. 193–195, Mar. 2005.

[14] P. Ödling, P. O. Börjesson, T. Magesacher, and T. Nordström, "An approach to analog mitigation of rfi," *IEEE Journal on Selected Areas in Communications*, vol. 20, no. 5, pp. 974–986, June 2002.

[15] T. H. Yeap, D. K. Fenton, and P. D. Lefebvre, "A novel common-mode noise cancellation technique for vdsl applications," *IEEE Transactions on Instrumentation and Measurement*, vol. 52, no. 4, pp. 1325–1334, Aug. 2003.

[16] A. H. Kamkar-Parsi, G. Bessens, M. Bouchard, and T. H. Yeap, "Wideband crosstalk interference cancelling on xdsl using adaptive signal processing and common mode signal," in *IEEE International Conference on Acoustics, Speech and Signal Processing (ICASSP)*, vol. 4, Montral, QUEBEC, May 2004, pp. 1045–1048.

[17] A. H. Kamkar-Parsi, M. Bouchard, G. Bessens, and T. H. Yeap, "A wideband crosstalk canceller for xdsl using common-mode information," *IEEE Transactions on Communications*, vol. 53, no. 2, pp. 238–242, Feb. 2005.

[18] T. Magesacher, S. Haar, and R. Zukunft, "Analysis of the noise environment in future twisted-pair access technologies," in *Emerging Technologies Symposium on 'Broadband Communications for the Internet Era'*, Dallas, USA, Sept. 2001.

[19] T. Magesacher, W. Henkel, T. Nordström, P. Ödling, and P. O. Börjesson, "On the correlation between common-mode and differential-mode signals," in *ETSI TM6/TD45*, Stockholm, SWEDEN, Sept. 2001.

[20] T. Magesacher, P. Ödling, P. O. Börjesson, W. Henkel, T. Nordström, R. Zukunft, and S. Haar, "On the capacity of the copper cable channel using the common mode," in *IEEE Global Telecommunications Conference (GLOBECOM)*, Taipei, TAIWAN, Nov. 2002.

[21] T. Magesacher, P. Ödling, J. Sayir, and T. Nordström, "Capacity of an extension of cover's two-look gaussian channel," in *IEEE International Symposium on Information Theory (ISIT)*, Yokohama, JAPAN, June 2003.

[22] T. Magesacher, P. Ödling, P. O. Börjesson, and T. Nordström, "Exploiting the common-mode signal in xdsl," in *European Signal Processing Conference (EUSIPCO)*, Vienna, AUSTRIA, Sept. 2004, pp. 1217–1220.

[23] B. Lee, "Binder mimo channels," Ph.D. dissertation, Stanford University, Oct. 2004.

[24] J. M. Cioffi, B. Lee, M. Mohseni, A. Leshem, and L. Youming, "Gdsl (gigabit dsl)," in *ANSI T1E1.4/2003-487R1*, Aug. 2004.

[25] T. Magesacher, W. Henkel, G. Taubck, , and T. Nordstrm, "Cable measurements supporting xdsl technologies," *Journal e&i Elektrotechnik und Informationstechnik*, vol. 199, no. 2, pp. 37–42, Feb. 2002.

[26] W. G. on Digital Subscriber Line Access, "Spectrum management for loop transmission systems," in *ANSI T1.417-2001*, 2001.

[27] K. Foster and J. Cook, "The radio frequency interference (rfi) environment for very high-rate transmission over metallic access wire-pairs," in *ANSI T1E1.4/95-020*, Mar. 1995.

[28] L. de Clerq, , M. Peeters, S. Schestraete, and T. Pollet, "Mitigation of radio interference in xdsl transmission," *IEEE Communications Magazine*, pp. 168–173, Mar. 2000.

[29] S. Galli and K. J. Kerpez, "Methods of summing crosstalk from mixed sources-part i: Theoretical analysis," *IEEE Transactions on Communications*, vol. 50, no. 3, pp. 453–461, Mar. 2002.

[30] K. J. Kerpez and S. Galli, "Methods of summing crosstalk from mixed sources-part ii: Performance results," *IEEE Transactions on Communications*, vol. 50, no. 4, pp. 600–607, Apr. 2002.

[31] C. Zeng and J. M. Cioffi, "Near-end crosstalk mitigation in adsl systems," *IEEE Journal on Selected Areas in Communications*, vol. 20, no. 5, pp. 949–958, June 2002.

[32] C. Valenti, "Next and fext models for twisted-pair north american loop plant," *IEEE Journal on Selected Areas in Communications*, vol. 20, no. 5, pp. 893–900, June 2002.